THE KOREAN JOURNAL OF QUATERNARY RESEARCH Vol. 20, No. 1, p. 9-27 (June, 2006)

The change of East Asian Monsoon to CO_2 increase

R. H. Kripalani[1], J. H. Oh[2]*, H. S. Chaudhari[2]

[1]Indian Institute of Tropical Meteorology, June, India
Integrated Climate System Modeling Laboratory
[2]Department of Environmental and Atmospheric Sciences
Pukyong National University, Busan, Korea

요약: 이 연구는 동아시아 (중국, 한국, 그리고 일본) 여름몬순과 그 변동성을 MME (multi-model ensemble)을 이용하여 IPCC AR4 (Intergovernmental Panel on Climate Change Fourth Assessment Report) 실험의22개 접합 기후모델 결과 자료로 분석하였다. 결과자료들은 사용 가능한 모든 모델의 평균값을 이용하였다.
여름 몬순 기간 동안 최대 강수를 가지는 연주기는 모델에 의해 모의되었으나 장마(Meiyu-Changma-Baiu) 강수밴드의 이동(북쪽)과 연관되어 7월에 나타나는 최소값은 모의하지 못했다. MME 강수 패턴은 북태평양 아열대 고기압과 장마전선대의 위치와 연관된 강수의 공간적 분포를 잘 나타내었다. 그러나 중국, 한반도, 그리고 일본의 동해와 인근 해역의 강수는 과소 예측되었다.
마지막으로 CO_2 농도 배증시나리오의 복사 강제에 대한 미래예측을 분석하였다. MME는 CO_2 농도가 배증될 때 동아시아지역에서 강수는 평균 7.8%로 나타났고, 5~10%의 변화폭을 보였다. 그러나 이러한 강수의 증가는 통계적으로 한반도와 일본, 그리고 인근 북중국 지역에서만 중요한 의미를 가진다. 강수 예측에서 나타난 변화는 아열대 고기압의 강도 변화에 비례하는 것으로 나타났다. 그리고 봄에서 초가을까지 여름 몬순의 지속기간이 길어짐을 확인하였다.

주요어: 기후변화, 동아시아 몬순

Abstract: The East Asian (China, Korea and Japan) summer monsoon precipitation and its variability are examined from the outputs of the 22 coupled climate models performing coordinated experiments leading to the Intergovernmental Panel on Climate Change Fourth Assessment Report (IPCC AR4) following the multi-model ensemble (MME) technique. Results are based on averages of all the available models.
The shape of the annual cycle with maximum during the summer monsoon period is simulated by the coupled climate models. However, models fail to simulate the minimum peak in July which is associated with northward shifts of the Meiyu-Changma-Baiu precipitation band. The MME precipitation pattern is able to capture the spatial distribution of rainfall associated with the location of the north Pacific subtropical high and the Meiyu-Changma-Baiu frontal zone. However precipitation over the east coast of China, Korea-Japan peninsular and the adjoining oceanic regions is underestimated.
Future projections to the radiative forcing of doubled CO_2 scenario are examined. The MME reveals an increase in precipitation varying from 5 to 10 %, with an average of 7.8 % over the East Asian region at the time of CO_2 doubling. However the increases are statistically significant only over the Korea-Japan peninsula and the adjoining north China region. The increase in precipitation may be attributed to the projected intensification of the subtropical high, and thus the associated influx of moist air from the Pacific to inland. The projected changes in the amount of precipitation are directly proportional to the changes in the strength of the subtropical high. Further a possible increase in the length of the summer monsoon precipitation period from late spring through early autumn is suggested.

Key Words: Climate Change East Asian Monsoon

* Corresponding author: Jai-Ho Oh, Email: jhoh@pknu.ac.kr

1. Introduction

Climate modeling groups around the world have been performing a set of coordinated 20th and 21st century climate change experiments, in addition to commitment experiments extending to the 22nd century for the Inter- governmental Panel on Climate Change Fourth Assessment Report (IPCC AR4).

The increased emissions of CO_2 have lead to the increase in heating of the earth (IPCC, 2001) and the simulated climate change is largely due to the radiative influence of CO_2. Here we analyze and examine transient and equilibrium runs under the 1% per year compounded increase in CO_2 until reaching double (IPCC AR4 experiment acronym '1pctto2x') and held constant thereafter. These transient runs are compared with the 20th century climate in coupled models (IPCC AR4 experiment acronym '20c3m'). The difference between the '1pctto2x' and '20c3m' experiments represents the projected changes at the time of CO_2 doubling.

The Asian region is characterized by high human population and economies tend to be highly vulnerable to changes in monsoon precipitation. Hence the variation in seasonal monsoon rainfall in the context of global warming is a critical issue to be investigated. Numerous studies have well documented that the Asian summer monsoon system can be divided into two subsystems: the South and the East Asian monsoon system which are to a greater extent independent of each other and, at the same time, interact with each other (e.g. Kripalani and Kulkarni, 2001; Ding and Chan, 2005). Analysis of the precipitation data under the IPCC AR4 experiments over the South Asian region have been recently reported (Kripalani etal., 2005a 2006).

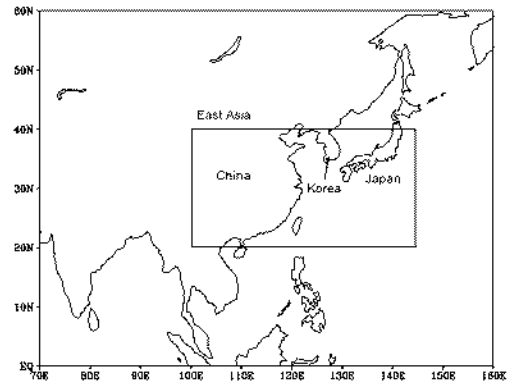

Fig. 1. The rectangular box indicates the region of analysis in this study.

In view of the above the 20th century simulated summer monsoon (June through August: JJA) precipitation over the East Asia (20-40° N, 100-145° E Fig.1) comprising of China, Korea and Japan and the adjacent oceanic region, for all the available models and runs are analyzed with respect to the annual cycles and the spatial patterns. Simulations are compared with the observed features. Precipitation projected at the time of CO_2 doubling is then investigated. Results based on averages of all available models i.e. multi-model ensemble (MME) technique are mostly presented. The aims of this study are to quantify the changes in summer precipitation over East Asia in response to doubled CO_2 and to determine the possible factors responsible for these changes.

2. Models, Data and Methodology

The IPCC standard output from coupled ocean-atmosphere GCMs (General Circulation Models) is collected and archived by the WGCM (Working Group on Coupled Models) Climate simulation panel and the Program for Climate Model Diagnosis and Inter-comparison (PCMDI) at the Lawrence Livermore National Laboratory, USA. The climate models along with the key references are listed in Table 1. Each model is identified by a simplified 3-letter abbreviation (Table 1). Other model characteristics such as horizontal resolutions (resolutions are given in approximate Gaussian grid: longitude- latitude up to first place of decimal), number of ensembles,

Table 1. Climate models,their versions and the key reference for each model. Each model is identified by a simplified 3-letter abbreviation.

Ser No	IPCC ID	Simplified Abbreviation	Country	Key Reference
1	BCC-CM1	bcc	China	Not available
2	BCCR-BCM2.0	bcr	Norway	Furevik et al. 2003
3	CGCM3.1	ccm	Canada	Flato et al. 2000
4	CNRM-CM3	cnr	France	Salas-Melia et al. 2006
5	CSIRO-MK3.0	csr	Australia	Gordon et al. 2002
6	GFDL-CM2.0	gf0	USA	Delworth et al. 2006
7	GFDL-CM2.1	gf1	USA	Delworth et al. 2006
8	GISS-AOM	gao	USA	Russell et al. 1995
9	GISS-EH	gih	USA	Schmidt et al. 2006
10	GISS-ER	gir	USA	Schmidt et al. 2006
11	FGOALS-g1.0	iap	China	Yu et al. 2004
12	INM-CM3.0	inm	Russia	Diansky & Volodon 2002
13	IPSL-CM4	ips	France	Marti et al. 2005
14	MIROC3.2 (hires)	mih	Japan	K-1 Model Developers 2004
15	MIROC3.2 (medres)	mim	Japan	K-1 Model Developers 2004
16	ECHO-G	miu	Germany/Korea	Legutke and Voss (1999)
17	ECHAM5/MPI-OM	mpi	Germany	Jungclaus et al. 2006
18	MRI-CGCM2.3.2	mri	Japan	Yukimoto et al. 2001
19	CCSM3	ncc	USA	Collins et al. 2006
20	PCM	ncp	USA	Washington et al. 2000
21	UKMO-HadCM3	ukc	UK	Jones et al. 2004
22	UKMO-HadGEM1	ukg	UK	Johns et al. 2005

Table 2. Characteristics of the climate models: Approximate Gaussian grid atmospheric resolution (lon x lat), Number of ensembles (20c3m, 1pctto2x), Convection schemes used (AS=Arakawa-Schubert, RAS=Relaxed Arakawa-Schubert, MF=Mass flux-based, MC=Moist Convection Adjustment) Flux corrections at the Ocean-Atmosphere interface (N=None, H=Heat, W=Water, M=Momentum). A dash (-) indicates information not available.

Ser No	Model	Approximate Resolution	Ensembles (20c, 1pc)	Convection Scheme	Flux Cor-rection
1	bcc	1.9 x 1.9	4, 1	-	-
2	bcr	2.8 x 2.8	1, 0	MF	N
3	ccm	3.7 x 3.7	1, 1	MC	HW
4	cnr	2.8 x 2.8	1, 1	MF	N
5	csr	1.9 x 1.9	1, 1	MC	N
6	gf0	2.5 x 2.0	3, 1	RAS	N
7	gf1	2.5 x 2.0	3, 1	RAS	N
8	gao	4.0 x 3.0	2, 0	MF	N
9	gih	5.0 x 4.0	5, 1	MF	N
10	gir	5.0 x 4.0	9, 1	MF	N
11	iap	2.8 x 3.0	3, 3	MF	N
12	inm	5.0 x 4.0	1, 1	MC	W
13	ips	3.7 x 2.5	1, 1	MC	N
14	mih	1.1 x 1.1	1, 1	AS	N
15	mim	2.8 x 2.8	3, 3	AS	N
16	miu	3.7 x 3.7	5, 1	MF	N
17	mpi	1.9 x 1.9	3, 3	MF	N
18	mri	2.8 x 2.8	5, 1	AS	HWM
19	ncc	1.4 x 1.4	8, 1	AS	N
20	ncp	2.8 x 2.8	4, 4	AS	N
21	ukc	3.7 x 2.5	2, 1	MF	N
22	ukg	1.9 x 1.2	1, 1	MF	N

convection schemes employed for precipitation parameterization and the flux corrections (if any) are tabulated in Table 2. There is a fairly large range in the horizontal resolution of the models varying from the highest ~1.1° longitude / latitude to the lowest 5° longitude by 4° latitude. More details of the coupled climate models are available at http://www-pcmdi.llnl.gov/ipcc/model_documentation/.

Given the relative success of MME technique in the field of dynamical seasonal forecasting, a similar strategy for climate scenarios is adopted here. Uncertainties could be reduced on smaller regional scales by the technique of multi-model averaging. To achieve the purposes of this study, data are analyzed over the East Asian region (Fig.1) based on averages of model ensembles: (i) Monthly average rainfall in mm/month averaged for all the grids to examine the annual cycle(ii) Summer season (JJA) average rainfall in mm at each grid point to examine the spatial patterns

Model results are compared with the observed data from Climate Prediction Center Merged Analysis Precipitation (CMAP; Xie and Arkin, 1997). The CMAP precipitation (obtained from the website ftp://ftpprd.ncep.noaa.gov) has a resolution of 2.5° longitude by 2.5° latitude. Based on the CMAP rainfall data for the 1981-2000 period, seasonal rainfall over the East Asian region (Fig. 1) during winter (DJF), spring (MAM), summer (JJA) and autumn (SON) is 178, 348, 542, 318 mm respectively. Thus a substantial contribution (~ 40 %) of the annual rainfall occurs during summer. The coefficient of variation (CV) during summer is 6.7 %.

For selected models the sea level pressure from the '20c3m' and the '1pctto2x' experiments is also examined to identify possible projected changes in the pressure patterns. Before the results of this study are discussed, a brief overview of the climate conditions and summer monsoon circulation over East Asia is presented in the next section.

3. Summer monsoon climate over East Asia

The East Asian summer monsoon is tropical and subtropical nature. The most prominent weather phenomenon during the summer monsoon is the quasi-stationary front extending from south China to southern Japan. This front called *Meiyu* in China, *Changma* in Korea and *Baiu* in Japan is located along the northern and northwest periphery of the north Pacific subtropical high (NPSH). The location, shape and strength of the NPSH greatly influence the East Asian climate (see Ding and Chan, 2005 and references therein). The westward (eastward) extension of the NPSH enhances (suppresses) monsoon activity. The westward displacement intensifies the low level jet at the northwest edge of this anticyclone resulting in transporting of large amount of water vapor into East Asia, in particular over the Yangtze River Basin. At the southern edge of this high is the west Pacific warm pool. The anomalous heating over the warm pool also influences the atmospheric circulation and precipitation distribution (e.g. Nitta, 1987; Lu, 2001; also see Kim et. al., 2002, Kripalani et. al., 2002; 2005 band references therein).

The seasonal march of the East Asian summer monsoon precipitation displays a distinct stepwise northward and northeastward advance, with abrupt northward jumps and stationary periods in between. The monsoon rain commences from early to mid-May over the Indo-China peninsular, and then it extends abruptly to the Yangtze River Basin and south Japan in early to mid-June and finally penetrates to North China, Korea, parts of Japan and adjoining ocean (e.g. Ding and Chan, 2005).

Two external forcings i.e. the Pacific sea surface temperatures (SSTs) related with the El Nino Southern Oscillation (ENSO) Indian Ocean SSTs related with the Indian Ocean Dipole/Zonal Mode and the snow cover over Eurasia and the Tibetan Plateau are believed to be contributing factors to the activity of the East Asian summer monsoon (e.g. Kripalani et al., 2002; 2005b Ding and Chan, 2005; Oh et al., 2005). However, the internal variability of the atmospheric circulation is also very important. In particular the NPSH plays a more important role (Ding and Chan, 2005). With this climatic background we analyze the contemporary and projected East Asian monsoon.

4. Simulations and projections

As recommended by the IPCC AR4 panel, the models' mean climate is defined based on the last twenty years (corresponding to 1981-2000 period) of the "all forcing 20th century runs" i.e. experiment designated as '20c3m'. Observed climatology is also based on the 1981-2000 period.

4.1 Annual Cycles

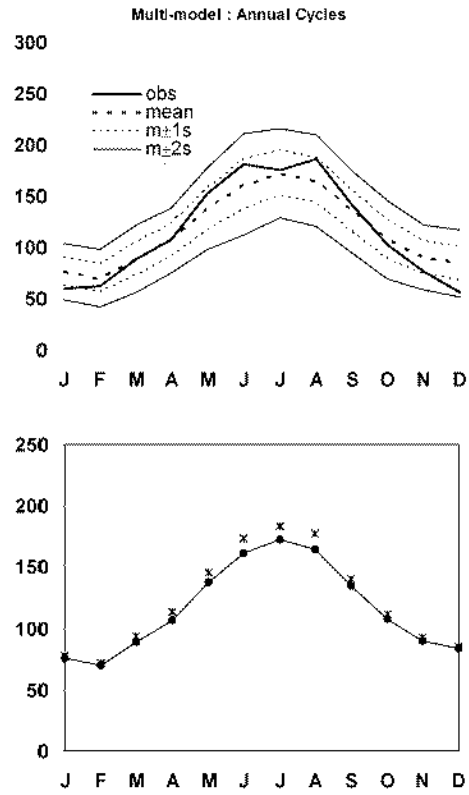

Fig. 2. Average monthly rainfall (mm/month) depicting the annual cycle (J=January ----- D=December). The average annual cycle based on all the models (mean: thick dashed curve), observed (obs: thick line), 1 (thin dashed curve) and 2 (thin continuous curve) standard deviation (m+/-s) limits are shown in the upper panel. The multi-model mean for the 20c3m (continuous line) and the 1pctto2x (dashed line) experiments are shown in the lower panel.

The CMAP (Xie and Arkin, 1997) average precipitation (mm) for each month, depicting the observed annual cycle is shown in Fig.2 (upper panel: thick line). Over the course of the annual cycle the precipitation shows a gradual increase from spring to summer with peak in July thereafter a gradual decrease

towards autumn. The precipitation in JJA is about 180–190 mm/month. However the observed precipitation shows a slight minimum in July and higher values in June and August. This could be related to the seasonal advace and withdrawal of the *Meiyu–Changma–Baiu* frontal zone. This frontal rain belt moves northward in sudden shifts with stationary periods in between as described in the previous section. It is likely that during the stationary period in July the monsoon activity is subdued resulting in lower precipitation in July compared to June and August.

The MME annual cycle (Fig.2 upper panel: thick dashed line) along with the 1 and 2 standard deviation limits (i.e. inter–model variability) are displayed in Fig.2 (upper panel). The simulated annual cycle resembles reasonably well the observed, but the simulation does not have peaks in June and August and the simulated precipitation is slightly underestimated from May through September. As will be seen later (section 4.2 Fig. 4) over major part of the East Asian domain, in particular the oceanic region, simulated precipitation is underestimated. The standard deviation of all the model simulations relative to the MME illustrates the inter–model variation. The inter–model variation is slightly larger during summer, implying larger diversity of the models in simulating summer monsoon precipitation.

The simulated (thick line) and projected (dotted line) annual cycles are shown in Fig.2 (lower panel).The projected annual cycle is based on the 20 years (years 61–80) centered (year 70) at the time of CO_2 doubling. Increase in precipitation throughout the year is projected, in particular from late spring through early autumn, implying the lengthening and strengthening of the Asian summer monsoon. From observed temperature data analysis over South Korea, Oh et al. (2004) have shown that summer has come earlier and lasts longer in the 1990s than inthe 1910s. The length of summer during 1990s was 109 days as against 87 days in the 1910s (Oh et al., 2004). Kitoh and Uchiyama (2006) also reported a significant delay in early summer rain withdrawal from Taiwan to the south of Japan under the SRES (Special Report on Emission Scenarios) A1B scenario. They also report an early withdrawal over south China and the Yangtze River Basin, but not significant due to inconsistent sign of the changes among the models. They further report that higher mean sea level pressure anomalies in the tropical western Pacific in the future may be related to these late withdrawals. Changes in onset dates are relatively short compared to those in the withdrawal dates (Kitoh and Uchiyama, 2006)

In summary analysis of simulated and projected annual cycles reveals an increase in summer precipitation and a possible lengthening of the summer rainy season from late spring through to early autumn.

4.2 Spatial Patterns

The major observed features of the summer monsoon rainfall distribution over the Asian regionshown by the CMAP data (Fig. 3) are as follows:

(i) Maximum rainfall (700−800 mm) over the region 20° −25° N up to 135° E and over the Korea−Japan peninsula

(ii) Minimum rainfall (100−200 mm) over the northwest sector of this region

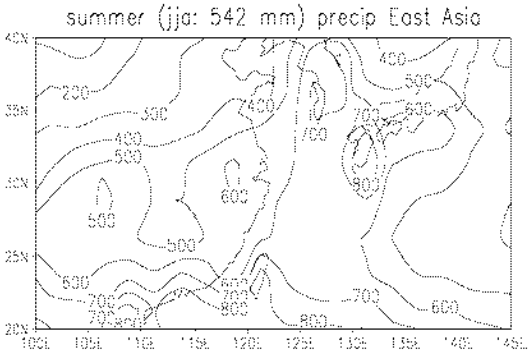

Fig. 3. Observed spatial pattern of seasonal summer monsoon (JJA) precipitation in mm as derived from the CMAP data set. The total seasonal precipitation is 542 mm over this region.

The heavy rainfall belts, south of 25° N and from southern China up to the Korea−Japan peninsular, may be related with the northward shifts of the *Meiyu−Changma−Baiu* front during summer. While the low rainfall over the eastern parts of the oceanic region compared to the western part may be related to the location of the NPSH. The easterly flow at the southern edge of this high will transport more moisture from the Pacific towards the west. The presence of the warm Kuroshio Current in the western Pacific also leads to the increase in precipitation.

To obtain the MME pattern the original model outputs are converted to the same resolution (2.5° longitude/latitude) by bi−linear interpolation method (http://badc.nerc.ac.uk/help/software/xconv/).

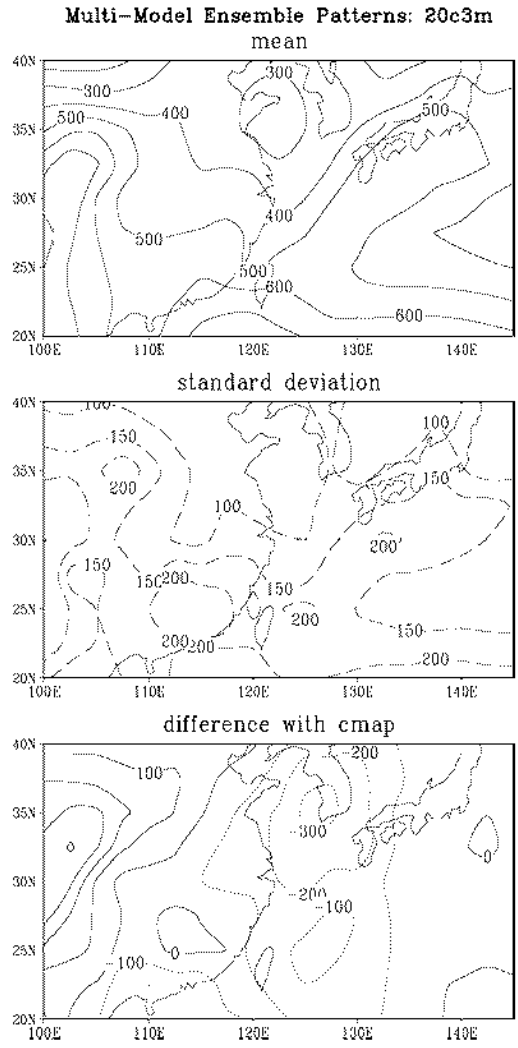

Fig. 4. Simulated MME pattern (upper panel) and the pattern of standard deviation (central panel) for all the models relative to the MME in mm. The difference (in mm) between MME and CMAP is illustrated in the lower panel.

The simulated spatial pattern is shown in Fig. 4 (upper panel). A comparison with Fig. 3 reveals that the multi−model ensemble is able to capture the major spatial features reasonably well. For an objective assessment about the inter−model variance,

Fig.4 (central panel) presents the standard deviation of the models relative to the MME. The pattern of standard deviation is similar to the mean multi-model pattern with higher deviations (~200 mm) among the models over regions of high rainfall and lower deviations (100-150 mm) in regions of low rainfall. Thus the inter-model variation of precipitation is about 2 times larger south of 30° N, than north of this latitude, indicating the larger diversity of the coupled models in simulating low latitude precipitation.

The difference between the MME and CMAP pattern reveals underestimation of precipitation over east coast of China, Korea-Japan peninsular and the adjoining oceanic regions (Fig.4 lower panel). Sun et al. (2006) also found dry biases over East China simulated by several models. Using a GCM, Zhang (1994) performed two simulations for the summer monsoon months, one with convection parameterization using a mass flux scheme and the other without convective parameterization. Significant effects on the monsoon circulation and its associated precipitation were reported. In the simulation with the mass flux convective parameterization, precipitation in the western Pacific decreased, together with a decrease in surface evaporation and wind speed. Besides the convective parameterization, others factors such as dynamics and thermodynamics could also be responsible for low precipitation. Zhang (1994) further showed that the monsoon circulation and precipitation distribution in the no-convection simulation are very similar to those in the simulation with moist convection adjustment scheme. He interpreted the precipitation decrease and the difference in the large-scale circulation with and without convective parameterization in terms of convective stabilization of the atmosphere by convection, using dry and moist static energy budgets. He showed that weakening of the low-level convergence in the western Pacific in the simulation with convection closely associated with the stabilization of the atmosphere by convection, mostly through drying of the lower troposphere; changes in low-level convergence leading to changes in precipitation. Thus the stabilization of the atmosphere inhibits the vertical motion and the low-level moisture convergence leading to suppressing precipitation. Incidentally 70 % of the models used here have employed either the mass-flux based convective parameterization scheme or the moist convective adjustment scheme (see Table 2). This may be a possible reason for the underestimation of precipitation over this region in particular over east coast of China, Korea-Japan peninsular and the adjoining west Pacific region (Fig. 4 lower panel).It is also likely that the dryness in East Asia is due to a poor representation of the dynamics, which is responsible for the moisture transport.

The projected spatial patterns (Fig. 5) are depicted as differences between the mean patterns at the time of CO_2 doubling (years 61-80 of the transient 1pctto2x runs) and the last 20-years of the control runs (20c3m runs). The differences between the simulated and projected patterns are tested by a two-tailed student's t-test. Shaded areas denote areas of significance. Maximum increases of 50 mm are projected over southern China, Japan and the adjoining oceanic regions (Fig. 5 upper panel).

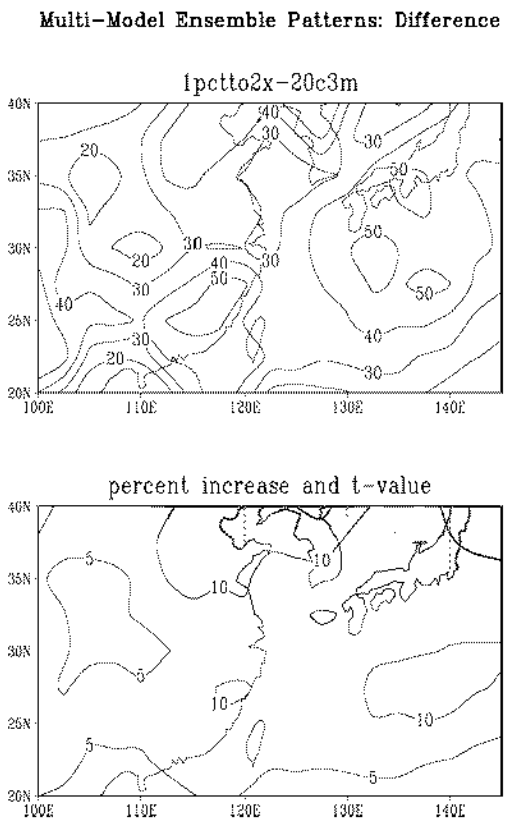

Fig. 5. Spatial patterns depicting the difference (1pctto2x-20c3m: upper panel) in mm and the percent increase in precipitation (lower panel). Light (dark) gray shading illustrates the significance at 5 (1) % level determined from the two-tailed Student's t-test.

The precipitation increases vary from 5 to 10 % (Fig. 5 lower panel). On the whole, summer precipitation increases by 7.8 % by the CO_2 doubling, which is higher than the observed CV (6.7 %). Note, however, that the increases are significant only over the region north of 32° N and east of 112° E (Fig. 5 lower panel: shaded areas).

Min et al. (2004) reported precipitation change in summer to be positive over all East Asia with maximum change of 30 % near the Korean peninsular and Yellow sea based on 4 selected models under IPCC SRES A2 and B2 scenarios. They reported an overall increase of 10.4% in summer precipitation over the East Asian region. Kimoto (2005) also reported mean precipitation increases of 10 % in 100 years especially in warm seasons with the SRES A1B and B1 scenarios over Japan. However, using an interactive atmosphere-soil-vegetation model, Chen et al. (2004) obtained an increase of about 20 % in annual rainfall in coastal areas of northern and central China, but only by 8 % in south China under the doubled CO_2 scenario. The precipitation increases vary from model to model and from one scenario to another.

Recent climate trends in the East Asian region during Baiu season of 1979-2003 show an increase inprecipitation along the Baiu frontal zone from southeast part of China up to Japan (Hirota et al., 2005). Observed rainfall during the 20th century has also shown an increase in summer precipitation. Using data for the 1906-2002 period over South Korea, Chung et al. (2004) noted an increase in precipitation. They attributed the changes in observed rainfall characteristics to the behavior of the Changma front. Su et al. (2006) also reported a positive trend in summer precipitation in the Yangtze region due to increase of rainstorm frequency during the 1960-2002 period.

In summary the MME technique projects an increase of summer precipitation by 7.8 % over the East Asian region. Over smaller spatial scales maximum increase (10 %) in precipitation is projected over the Korea-Japan peninsula and the adjoining North China

region. We now examine the impact of stabilized CO_2 after attaining double concentration.

4.3 Impact of fixed CO_2 after doubling

Time series of average summer monsoon rainfall are prepared by averaging the outputs of 3 models (*ccm, inm, mpi*), because only for these 3 models control runs are available for 130 years and transient runs under the CO_2 doubling scenario for 220 years. A plot of these two series is shown in Fig. 6. The solid line super-imposed on the inter-annual fluctuations is a smoothed curve using 21-year running mean low-pass filter.

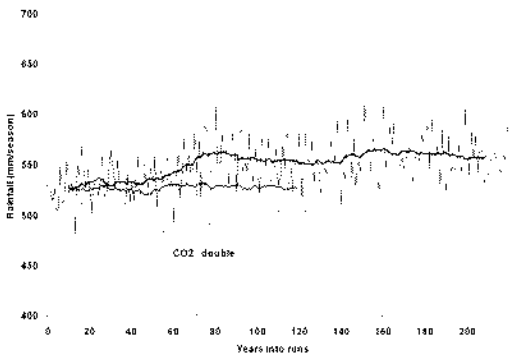

Fig. 6. Time series plot (average for ccm, in mand mpi models) of the mean JJA rainfall for the 20c3m (dotted line) and the 1pctto2x (continuous line) experiments. The solid line super- imposed on the inter-annual variations is a smoothed 21-year low pass filter. The vertical line at year 70 indicates the CO_2 doubling period. X-axis denotes the years and Y-axis the seasonal precipitation in mm.

This time series reveals a gradual increase in precipitation initially and a rapid increase from the year 40 until the time of CO_2 doubling (year 70). During the period CO_2 held constant and allowed to stabilize, there is some indication of slight increase in precipitation for a decade or so and remains constant thereafter, indicating a state of equilibrium. This suggests that the warming associated with the increase in CO_2 results in more evaporation, more moisture in the atmosphere, ultimately resulting in more precipitation. However the changes in precipitation might stabilize once the increases in CO_2 emissions are controlled.

5. Discussion: possible mechanisms for precipitation increase

Both the oceans and the atmosphere are warming as greenhouse gases build in the atmosphere. Warmer tropical SSTs with increased greenhouse gases produce relatively large increases in water vapor due to increased evaporation and consequently a general increase in tropical precipitation. At high latitudes, in addition to increases in water vapor producing more precipitation in regions of climatological moisture convergence, advection associated with changes in atmospheric circulation produces a large precipitation increase over several regions of the globe including the east coast of Asia (Hu et al., 2000; Meehl et al., 2005).

Several recent studies using the IPCC AR4 scenario have identified possible causes for the increase in summer precipitation over East Asia. Kimoto (2005) attributes the increased activity of East Asian monsoonal rain band to the strengthening of the anticyclone cells and inflow of subtropical moist air. Another possible cause for the increase in summer precipitation is an El Nino-like SST pattern in the future due to the increase in SST in

the eastern equatorial Pacific (Boer et al., 2004; Kurihara et al., 2005). Thus the SST change around the equatorial Pacific region will resemble that of an El Nino event. During such an event, the subtropical high pressure to the south of Japan intensifies, due to the shift of warm water over the western Pacific towards east. Along the rim of the high-pressure anomaly precipitation is projected to increase due to the intensified horizontal flux of water vapor. The areas falling in the region of intensified water vapor flux from the southwest direction will receive increased precipitation (Kurihara et al., 2005).

Tanaka et al. (2005) compared the intensities and trends of Hadley, Walker, and Monsoon Circulations of the IPCC 20th century simulations and for the 21st century projections, using upper troposphere velocity potential data. Significantly weaker biases in Walker and Monsoon circulations for the JJA climate in the IPCC 20th century simulations were noted. Analyses of the IPCC 21st century projections to investigate the trends of these tropical circulations in response to the projected global warming - showed that Hadley, Walker and Monsoon circulations are weakened by 9, 8, and 14 % respectively by the late 21stcentury according to the ensemble mean of the IPCC model projections (Tanaka et al., 2005). A contradictory fact of increasing Indian monsoon rainfall due to the global warming was explained by the increasing precipitable water in the monsoon area, despite the weakening monsoon circulation in the warmer than present climate (Kitoh et al., 1997).

Min et al. (2004) examined future climate changes over East Asia using selected coupled models based on IPCC SRES A2 and B2 scenarios. The overall projection results from MMEs show that East Asia will experience wetter climate in the 21st century. Spatial patterns indicate that precipitation increases are larger over continental area than the oceanic area. Climate change over East Asia has a characteristic seasonal dependence, with larger increases of summertime precipitation (Min et al., 2004, 2006).

Ueda et al. (2006) examined the response of the Asian summer monsoon (ASM) to a transient increase in future anthropogenic radiative forcing by multi-model global warming experiments. Most models show that in Asia the summer monsoon rainfall increases significantly with global warming. Enhanced moisture transport over the ASM region, associated with the increased moisture source from the warmer Indian Ocean, leads to larger moisture flux convergence, which is responsible for the intensification of the mean rainfall. Pronounced warming over the tropics in the middle-to-upper troposphere causes a reduction in the meridional thermal gradient in the Asian region, which is consistent with the weakened monsoon circulation and eastward shift of the Walker circulation (Ueda et al., 2006).

In summary the above studies indicate the possible intensification of the subtropical high and the associated moisture flux towards the land areas as a factor for increase in summer precipitation over East Asia in the warming condition. Based on selected models the impact of CO_2 doubling is examined on the NPSH. Three representative models with varying percent changes in precipitation are selected. While model *cnr* projects a minimum

change of −0.6 %, model *ukc* projects a maximum increase of 14 %. Model *mih* projects an increase of 4.8 %.

6. Impact on North Pacific Subtropical High

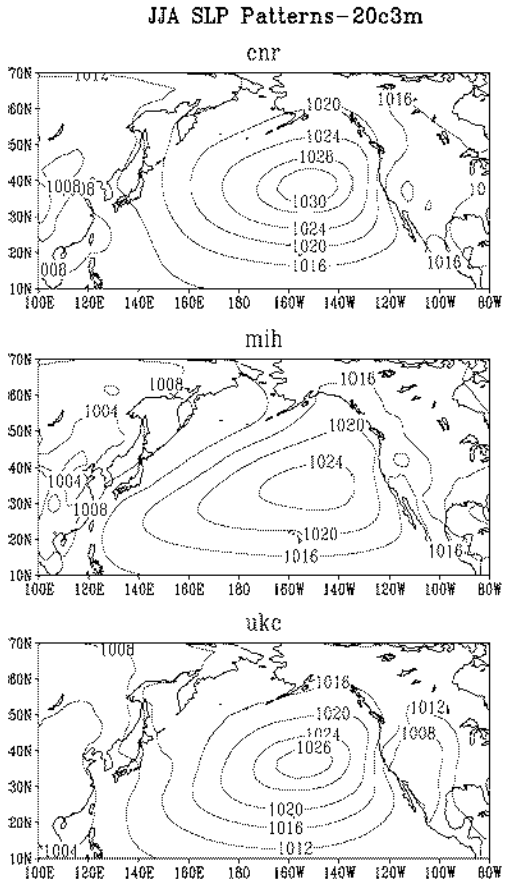

Fig. 7. Simulated sea level pressure (hPa) patterns by the three models: cnr (upper panel), mih (central panel) and ukc (lower panel).

The simulated spatial pattern and the location of the NPSH (30−40° N, 160−140° W) are well captured by these models (Fig. 7).

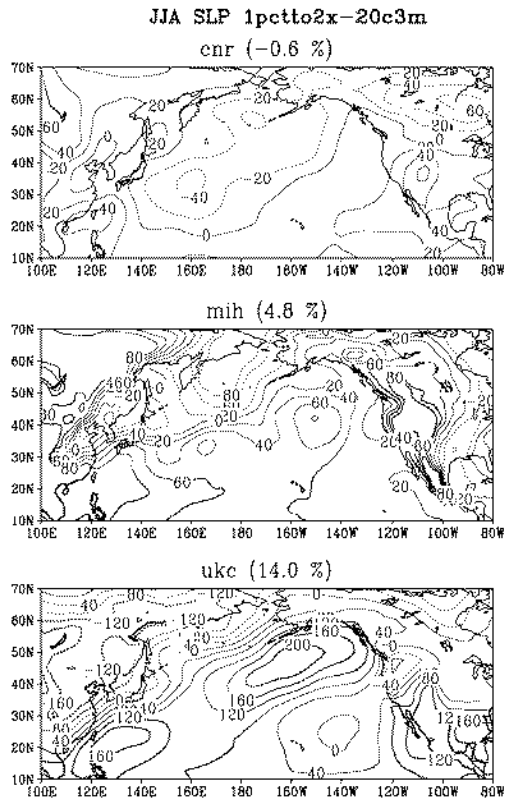

Fig. 8. Projected sea level pressure patterns for the three models (cnr, mih and ukc) as differences (1pctto2x−20c3m) in units of Pa (Pascals; 100 Pa=1 hPa i.e. hectapascals). Light (dark) gray shading illustrates the significance at 5 (1) % level. Model abbreviation and the percent increase in precipitation for the East Asian region areshown on top of each panel.

Projected SLP patterns are depicted as differences between the 1pctto2x and 20c3m runs (Fig. 8). These composite differences are also tested by the t−test. Shaded areas denote areas of significance. The negative anomalies (−0.2 to −0.4 hPa) for the *cnr* model over the Pacific indicates weakening of the NPSH, however the changes are insignificant. This model projects an overall decrease in summer

precipitation. However, an intensification of the NPSH with anomalies of the order of 0.4 to 0.6 hPa is indicated for the *mih* model. The negative anomalies from east coast of China up to the Korea-Japan peninsular may indicate intensification of the *Meiyu-Changma-Baiu* front. While the changes over the western edge of the NPSH appear significant, changes associated with the front are insignificant. This model shows an overall increase of 4.8%. The maximum intensification of the NPSH is also projected by *ukc* (1.6 to 2.0 hPa). Besides the intensification the NPSH is also projected to extend westwards (anomalies of 1.6 hPa around 20° N 130° E). The extension acts conducive for monsoon rainfall over East Asia as discussed in section 3. Again the negative anomalies from south China up to the Korea-Japan peninsula may amplify intensification of the *Meiyu-Changma-Baiu* front. The changes in the NPSH and the frontal zone are significant. Thus the projected changes in the amount of precipitation are directly proportional to the projected changes in the strength and shape of the NPSH, and possibly to the intensification of the *Meiyu-Changma-Baiu* front.

7. Summary

Some basic rainfall features over East Asia simulated during the 20th century by the coupled climate models in the IPCC AR4 database are investigated. Realistic simulation of the precipitation fields over regional scales is a very challenging task. Even though the coupled climate modeles used in this study did not prescribe SSTs to simulate pre-industrial climate they perform reasonably well in simulating the regional precipitation characteristics. Most of these newest generations of models do not employ flux adjustments, yet the rates of "climate drift" they exhibit are within the bounds for useful model simulation on time scales of a century or more. These developments represent significant progress in the state of the art of climate modeling since the second and third IPCC reports (Covey et al., 2003). An overall summary of the analysis undertaken in this study is as follows:

(i) The MME annual cycle resembles the observed reasonably well with maximum during summer monsoon period. However, models are unable to capture the minimum in July with peaks in June and August associated with the northward shifts of the *Meiyu-Changma-Baiu* frontal zone. The inter-model variation is slightly larger during summer, implying larger diversity of the models in simulating summer monsoon precipitation.

(ii) The broad spatial summer monsoon precipitation pattern is well captured including the *Meiyu-Changma -Baiu* frontal zone and the NPSH. However results reveal underestimation of precipitation during summer, in particular over the east coast of China, Korea-Japan peninsular and the adjoining west Pacific oceanic region. This could be related with the mass-flux based moist convective adjustment schemes employed by majority of the models for precipitation parameterization. The inter-model variation of precipitation is about 2 times stronger south of 30° N, than north of this latitude, indicating the larger diversity of the coupled models in simulating low latitude precipitation.

The MME technique suggests significant increases in precipitation of about 10 % over Korea-Japan peninsular and the adjoining north China region and as a whole, precipitation is projected to increase by 7.8 %, which is higher than the observed CV (6.7 %). The projected changes in summer precipitation are associated with the projected changes in the NPSH. Increase in the amount of precipitation is directly proportional to the increase in the strength of the NPSH and possibly to the intensification of the *Meiyu-Changma-Baiu* front. The length of the rainy summer season is projected to elongated. The lengthening of the summer monsoon period could have implications for water resources management and for adapting to possible new agricultural practices. The stabilization run indicates that the changes in precipitation could be stabilized if the emissions in CO_2 are controlled.

Acknowledgements

We acknowledge the international modeling groups for providing their data for analysis, the Program for Climate Model Diagnosis and Inter-comparison (PCMDI) for collecting and archiving the model data, the JSC/CLIVAR Working Group on Coupled Modeling (WGCM) and their Coupled Model Inter- comparison Project (CMIP) and Climate Simulation Panel for organizing the model data activity, and the IPCC WG1 TSU for technical support. The IPCC Data Archive at Lawrence Livermore National Laboratory is supported by the Office of Science, U.S. Department of Energy. Thanks are due to Pukyong National University for providing all the facilities. R.H. Kripalani was supported by the Korean Federation of Science and Technology Societies and H.S. Chaudhari was supported by Ph.D. studentship program for foreigners of Korea Science and Engineering Foundation.This work was funded by the Korea Meteorological Administration Research and Development Program under Grant CATER (Center for ATmospheric sciences and Earthquake Research) 2006-1101.

REFERENCES

Boer GJ, Yu B, Kim S-J, Flato G, (2004) Is there observational support for an El Nino-like pattern of future global warming?, Geop Res Lett 31: L06201, doi:10.1029/2003GL018722

Chen M, Pollard D, Barron EJ (2004) Regional climate change in East Asia simulated by an interactive atmosphere-soil-vegetation model. J Clim 17: 557-572

Chung Y-S, Yoon M-B, Kim H-S (2004) On climate variations and changes observed in South Korea. Clim Change 66: 151-161

Collins WD, Bitz CM, Blackmon ML, Bonan GB, Bretherton CS, Carton JA, Chang P, Doney SC, Hack JJ, Henderson TB, Kiehl JT, Large WG, McKenna DS, Santer BD, Smith RD (2006) The Community Climate System Model: CCSM3. J Clim (in press)

Covey C, AchutaRao KM, Cubasch U, Jones P, Lambert SJ, Mann ME, Phillips TJ, Taylor KE (2003) An overview of results from the Coupled Model Inter-comparison Project. Glob Planet Change 37: 103-133

Delworth TL, Broccoli AJ, Rosati A, Stouffer RJ, Balaji V, Beesley JA, Cooke WF, Dixon KW, Dunne J, Dunne KA, Durachta JW, Findell KL, Ginoux P, Gnanadesikan A, Gordon CT, Griffies SM, Gudgil R, Harrison MJ, Held IM, Hemler RS, Horowitz LW, Klein SA, Knutson TR, Kushner PJ, Langenhorst AR, Lee HC, Lin SJ, Lu J, Malyshev SL, Milly PCD, Ramaswamy V, Russel J, Schwarzkopf MD, Shevliakova E, Sirutis JJ, Spelman MJ, Stern WF, Winton M, Wittenberg AT, Wyman B, Zeng F, Zhang R (2006) GFDL's CM2 Global coupled climate models -Part 1: Formulation and simulation characteristics. J Clim 19: 643-674

Diansky NA, Volodin EM (2002) Simulation of present-day climate with a coupled Atmosphere-Ocean general circulation model. Izv Atmos Ocean Phys (Engl. Transl.) 38: 732-747

Ding Y, Chan JCL (2005) The East Asian summer monsoon: an overview. Met Atmos Phys 89: 117-142

Flato GM, Boer GJ, Lee WG, McFarlane NA, Ramsden D, Reader MC, Weaver AJ (2000) The Canadian Centre for Climate Modeling and Analysis of Global Coupled Model and its climate. Clim Dyn 16: 451-467

Furevik T, Bentsen M, Drange H, Kindem IKT, Kvamsto NG, Sorteberg A (2003) Description and evaluation of the Bergen Climate Model: ARPEGE coupled with MICOM. Clim Dyn 21: 27-51

Gordon HB, Rotstayn LD, McGregor JL, Dix MR, Kowalczyk, O'Farrell SP, Waterman LJ, Hirst AC, Wilson SG, Collier MA, Watterson IG, Elliott TI (2002) The CSIRO Mk3 Climate System Model (Electronic publication). Asoendale: CSIRO Atmospheric Research Technical Paper No. 60, 130pp

Hirota N, Takahashi M, Sato N, Kimoto M (2005) Recent climate trends in the East Asia during the Baiu season of 1979-2003. SOLA 1: 137-140

Hu Z-Z, Latif M, Roeckner E, Bengtsson L (2000) Intensified Asian summer monsoon and its variability in a coupled model forced by increasing greenhouse concentrations. Geophys Res Lett 27: 2681-2684

IPCC (2001) Climate Change 2001: The Scientific Basis. Contribution of Working Group I to the Third Assessment Report of the Intergovernmental Panel on Climate Change (Houghton JT, Y Ding, DJ Griggs, M Noguer, PJ van der Linden, X Dai, K Maskell, and CA Johnson (eds.)). Cambridge University Press, Cambridge, United Kingdom and New York, NY, USA, 881 pp

Johns T, Durman C, Banks H, Roberts M,McLaren A, Ridley J, Senior C, Williams K, Jones A, Keen A, Rickard G, Cusack S, Joshi M, Ringer M, Dong B, Spencer H, Hill R, Gregory J, Pardaens A, Lowe J, Bodas-Salcedo A, Start S, Searl Y (2005) HadGEM1-Model description and analysis of preliminary experiments for the IPCC 4th Assessment Report. Hadley Centre Technical Note 55, UK Met Office, 74 pp

Jones C, Gregory J, Thorpe R, Cox P, Murphy J, Sexton D, Valdes H (2004) Systematic optimization and climate simulation of FAMOUS, a fast version of HADCM3. Hadley Centre Technical Note 60, 33 pp

Jungclaus JH, Botzet M, Kaak H, Keenlyside N, Luo JJ, Latif M, Marotzke J, Mikolajewicz U, Roeckner E (2006) Ocean circulation and tropical variability in the AOGCM ECHAM5/MPI-OM. J Clim (in press)

K-1 Model Developers (2004) K-1 Coupled GCM (MIROC) description. K-1 Tech Report No. 1, Center for Climate System Research, University of Tokyo, National Institute for Environmental Studies, Frontier Research Center for Global Change (Hasumi and Emori eds), 39pp

Kim BJ, Kripalani RH, Oh JH, Moon SE (2002) Summer monsoon rainfall patterns over South Korea and associated circulation features. Theor Appl Climatol 72: 65-74.

Kimoto M (2005) Simulated change of the East Asian circulation under global warming scenario. Geophys Res Lett 32: doi: 10.1029/2005GL023383

Kitoh A, Uchiyama T (2006) Changes in onset and withdrawal of the East Asian summer rainy season by multi-model global warming experiments. J Meteor Soc Japan 84: (in press)

Kitoh A, Yukimoto S, Noda A, Motoi T (1997) Simulated changes in the Asian summer monsoon at times of increased atmospheric CO2. J Meteor Soc Japan 75: 1019-1031

Kripalani RH, Kim BJ, Oh JH, Moon SE (2002) Relationship between Soviet snow and Korean rainfall. Int J Climatol 22: 1313-1325

Kripalani RH and Kulkarni A (2001) Monsoon rainfall variations and tele-connections over south and East Asia. Int J Climatol 21: 603-616

Kripalani RH, Kulkarni A and Sabade SS (2005a) South Asian monsoon precipitation variability: Coupled climate model projections under IPCC AR4. CLIVARExchanges 10(3): 13-15

Kripalani RH, Oh JH, Kulkarni A, Sabade SS, Chaudhari HS (2006) South Asian summer monsoon precipitation variability: Coupled climate model simulations and projections under IPCC AR4. Theor Appl Climatol (accepted)

Kripalani RH, Oh JH, Kang JH, Sabade SS, Kulkarni A (2005b) Extreme monsoons over East Asia: Possible role of Indian Ocean Zonal Mode. Theor Appl Climatol 82: 81-94

Kurihara K, Ishihara K, Sasaki H, Fukuyama Y, Saitou H, Takayabu I, Murazaki K, Sato Y, Yukimoto S, Noda A (2005) Projection of climate change over Japan due to global warming by high-resolution Regional Climate Model in MRI. SOLA 1: 97-100

Legutke S, Voss R (1999) The Hamburg atmosphere-ocean coupled circulation model ECHO-G. DKRZ Technical Report No. 18, Deutsches Klimarechenzentrum, Hamburg, Germany, 62 pp

Lu RY (2001) Inter-annual variability of the summertime north Pacific subtropical high and its relation to atmospheric convection over the warm pool. J Met Soc Japan 79: 771-783

Marti O, Braconnot P, Bellier J, Benshile R, Bony S, Brockmann P, Cadulle P, Caubel A, Denvil S, Dufresne JL, Fairhead L, Filiberti MA, Fichefet T, Friedlingstein P, Grandpeix JY, Hourdin F, Krinner G, Levy C, Musat I, Talandier C (2005) The new IPSL climate system model: IPSL-CM4. Institut Pierre Simon Laplace, Paris, 86pp

Meehl GA, Arblaster JM, and Tebaldi C (2005)Understanding future patterns of increased precipitation intensity in climate model simulations. Geophys Res Lett 32: doi: 10.1029/2005 GL023680

Min S-K, Legutke S, Cubasch U, Kwon W-T, Oh J-H, Schlese M (2006) East Asian climate change in the 21st century as simulated by the coupled climate model ECHO-G under IPCC SRES scenarios. J Meteor Soc Japan (in press)

Min S-K, Park E-H and Kwon W-T (2004)Future projections of East Asian Climate Change from multi-AOGCM ensembles of IPCC SRES scenario simulations. J Meteor Soc Japan 82: 1187-1211

Nitta T (1987) Convective activities in the tropical western Pacific and their impacts on the northern summer circulation. J Met Soc Japan 65: 165-171.

Oh JH, Chaudhari HS, Kripalani RH (2005) Impacts of IODM and ENSO on the East Asian monsoon: Simulation through NCAR Community Atmospheric Model. Korean J Agri Forest Meteor 7: 240-249

Oh JH, Kim T, Kim MK, Lee SH, Min SK and Kwon WT (2004)Regional climate simulation for Korea using dynamic downscaling and statistical adjustment. J Meteor Soc Japan 82: 1629-1643.

Russell GL, Miller JR and Rind D (1995) A coupled atmosphere-ocean model for transient climate change studies. Atmos-Ocean 33: 683-730.

Salas-Melia D, Chauvin F, Deque M, Douville H, Gueremy JF, Marquet P, Planton S, Royer JF and Tyteca S (2006) Description and validation of the CNRM-CM3 global coupled model. Clim Dyn (in press)

Schmidt GA, Ruedy R, Hansen JE, Aleinov I, Bell N, Bauer M, Bauer S, Cairns B, Canuto V, Cheng Y, DelGenio A, Faluvegi G, Friend AD, Hall TM, Hu Y, Kelley M, Kiang NY, Koch D, Lacis AA, Lerner J, Lo KK, Miller RL, Nazarenko L, Oinas V, Perlwitz Jan, Perlwitz Judith, Rind D, Romanou A, Russel GL, Sato M, Shindell DT, Stone PH, Sun S, Tausnev N, Thresher D and Yao MS (2006) Present day atmospheric simulations using GISS ModelE: Comparison to in-situ, satellite and reanalysis data. J Clim (in press)

Su BD, Jiang T and Jin WB (2006)Recent trends in observed temperature and precipitation extremes in the Yangtze River basin, China. Theor Appl Climatol 83: 139-151

Sun Y, Solomon S, Dai A , Portmann R (2006)How often does it rain? J Clim 19: 916-934

Tanaka HL, Ishizaki N and Nohara D (2005) Intercomparison of the intensities and trends of Hadley, Walker and Monsoon Circulations in the Global Warming Projections. SOLA 1: 77-80

Ueda H, Iwai A, Kuwako K and Hori ME 2006: Impact of anthropogenic forcing on the Asian summer monsoon as simulated by 8 GCMs. Geophys Res Lett 33: doi:10.1029/ 2005 GL025336

Washington WM, Weatherly JW, Meehl GA, Semtner Jr. AJ, Bettge TW, Craig AP, Strand Jr. WG, Arblaster J, Wayland VB, James R and Zhang Y (2000) Parallel climate model (PCM) control and transient simulations. Clim Dyn 16: 755-774

Xie P and Arkin PA (1997) Global precipitation: a 17-year monthly analysis based on gauge observations, satellite estimates and numerical model outputs. Bull Amer Meteor Soc 78: 2539-2558

Yu Y, Zhang X and Guo Y (2004) Global coupled ocean-atmosphere general circulation models in LASG/IAP. Adv Atmos Sc 21: 444-455

Yukimoto S, Noda A, Kitoh A, Sugi M, Kitamura Y, Hosaka M, Shibata K, Maeda S and Uchiyama T (2001) The new Meteorological Research Institute Coupled GCM (MRI-CGCM2)-Model climate and variability. Papers in Meteorology and Geophysics 51:47-88

Zhang GJ (1994) Effects of cumulus convection on the simulated monsoon circulation in a General Circulation Model. Mon Wea Rev 122: 2022-2038

투 고 일: 2006. 4. 12.
심 사 일: 2006. 4. 24.
심사완료일: 2006. 5. 15.

R.H. Kripalani
Indian Institute of Tropical Meteorology, June, India Integrated Climate System Modeling Laboratory

J.H. Oh and H.S. Chaudhari
Department of Environmental and Atmospheric Sciences, Pukyong National University, Busan 608-737, South Korea